Low thermal conductive chalcogenides for high performance thermoelectric energy conversion

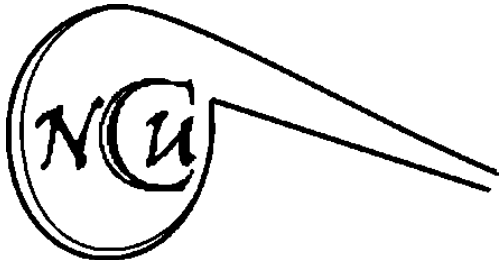

Kanishka Biswas

New Chemistry Unit

Jawaharlal Nehru Centre for Advanced Scientific Research (JNCASR)

Bangalore, India

kanishka@jncasr.ac.in

Thermoelectrics (TE)

The thermoelectric effect is the direct conversion of temperature differences to electric voltage and vice versa.

Seebeck Effect

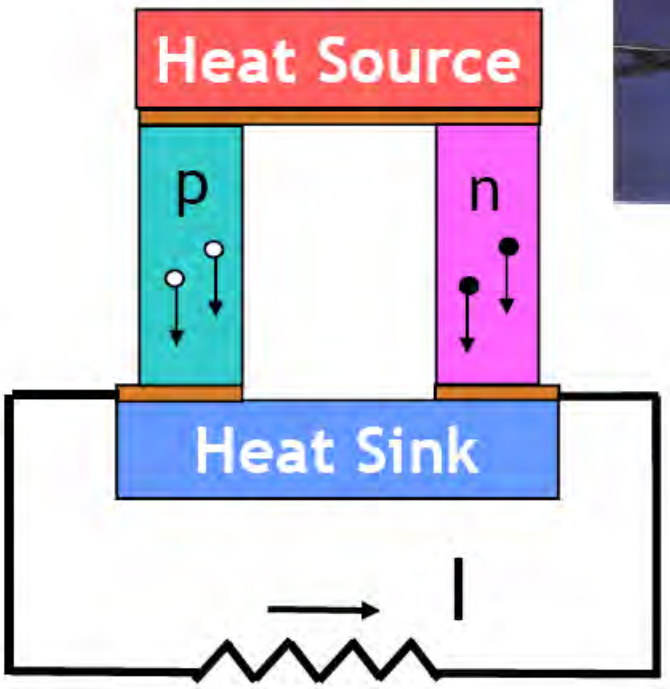

Power Generation Mode

"Electricity from waste-heat"

Peltier Effect

Refrigeration Mode

"Refrigeration without moving parts and chemical refrigerant"

Importance of Thermoelectrics

Total energy consumption

India (2015)

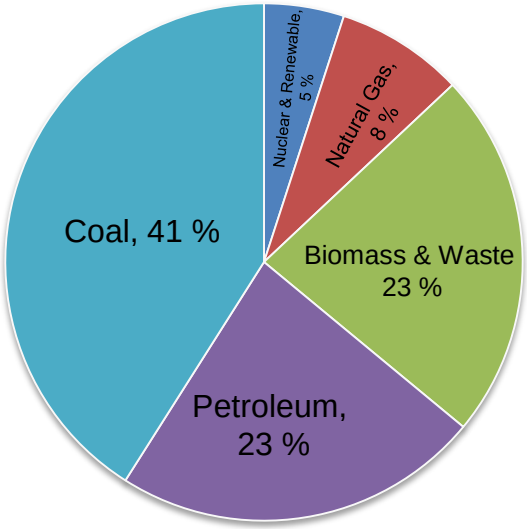

World (2015)

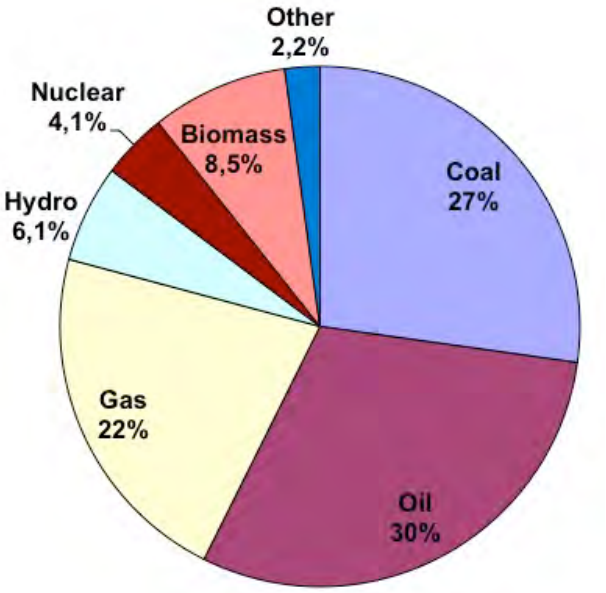

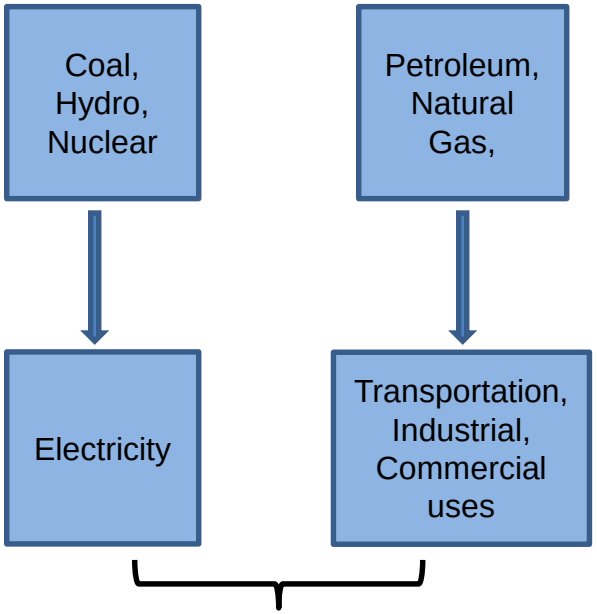

65 % of utilized energy rejected as waste heat

With about ~65 % of the utilized energy being lost as waste heat.
~20 % conversion to the useful form can have significant impact on overall energy utilization.

Thermoelectric materials allow the direct conversion between thermal and electrical energy.

Applications

Direct Heat to Electricity Conversion

Waste Heat Recovery/Power generation

- Large scale: Power plant (Chemical/thermal/Nuclear)
- Medium scale: Automobile

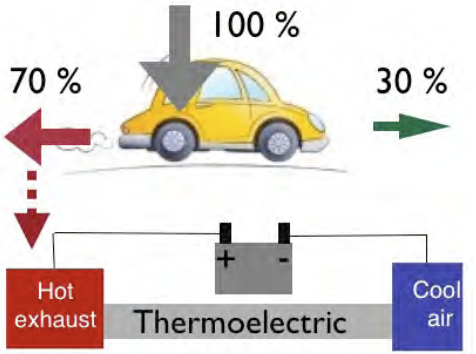

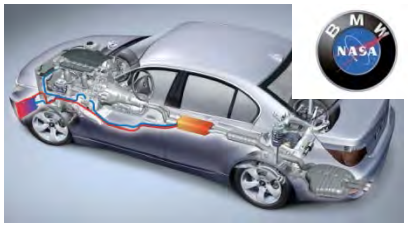

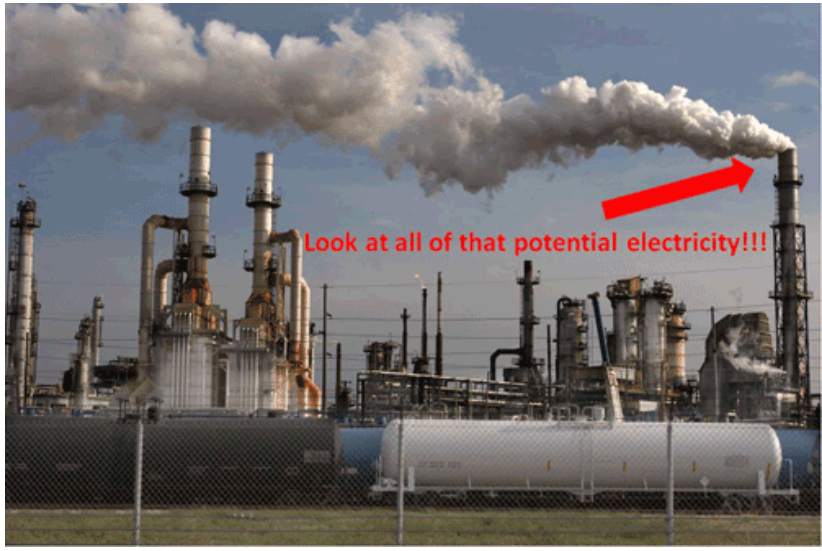

Space power generation

Solar-thermoelectrics

Cooling/Refrigeration

- Commercial cooler/warmer
- Spot cooling: microprocessor, laser diode
- Luxury vehicle: Cool/warm seat

The Mars Science Laboratory rover, Curiosity, is powered by its Radioisotope Thermoelectric Generator.

JPL-Caltech/NASA

Thermoelectric material

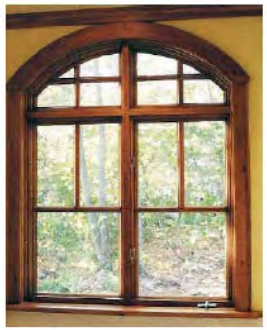

Glass

Low thermal conductivity

+

Metal

High electrical conductivity

+

Semiconductor

High Seebeck

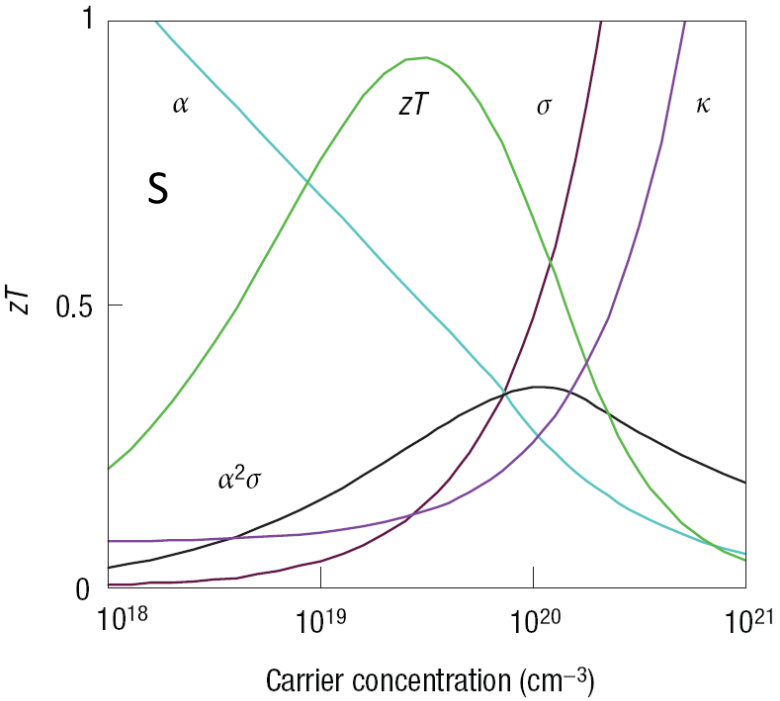

G. J. Snyder and E. S. Toberer, ***Nat. Mater.*** 2008, **7,** 105-114.

Seebeck Coefficient

Electrical conductivity

$$ZT = \frac{S^2\sigma}{\kappa}.T$$

Thermal conductivity (electrical + lattice)

Best thermoelectric materials: Highly doped narrow band gap semiconductor eg. Bi_2Te_3, PbTe .

Decoupling of electrical and phonon transport is essential for thermoelectrics

State of art thermoelectric bulk materials

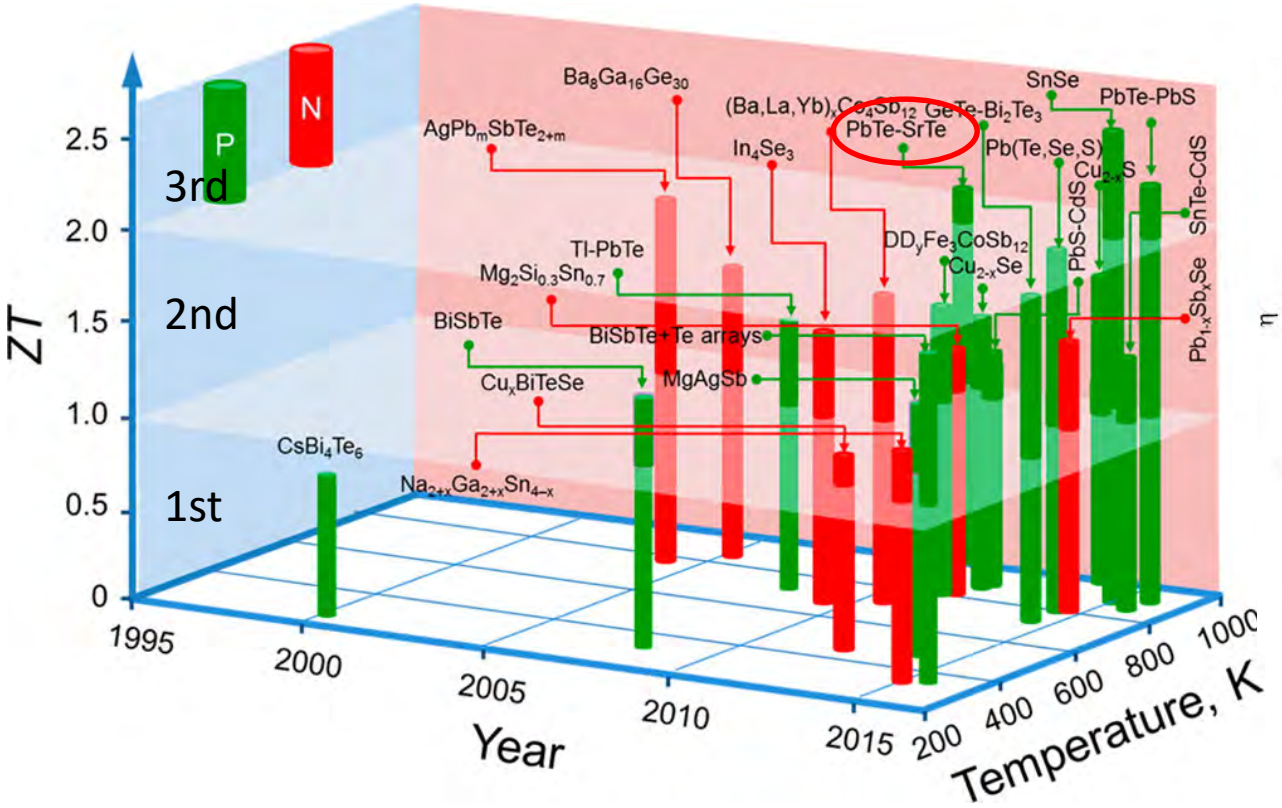

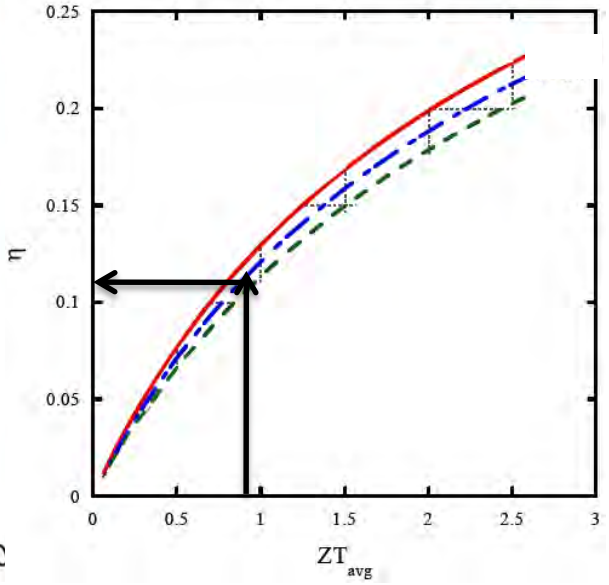

Commercial materials in market
η = 10 % with ZT of ≈ 1

$$\eta = \frac{\Delta T}{T_{hot}} \frac{\sqrt{1+ZT_{avg}}-1}{\sqrt{1+ZT_{avg}}+\frac{T_{cold}}{T_{hot}}}$$

G. Tan, L. D. Zhao and M. G. Kanatzidis, ***Chem. Rev.*** 2016, **116,** 12123.

Pb-free high performance materials are desired for mass-market applications

$$ZT = \frac{S^2\sigma}{\kappa}T$$

Bulk nanostructured thermoelectric materials

Decrease the thermal conductivity

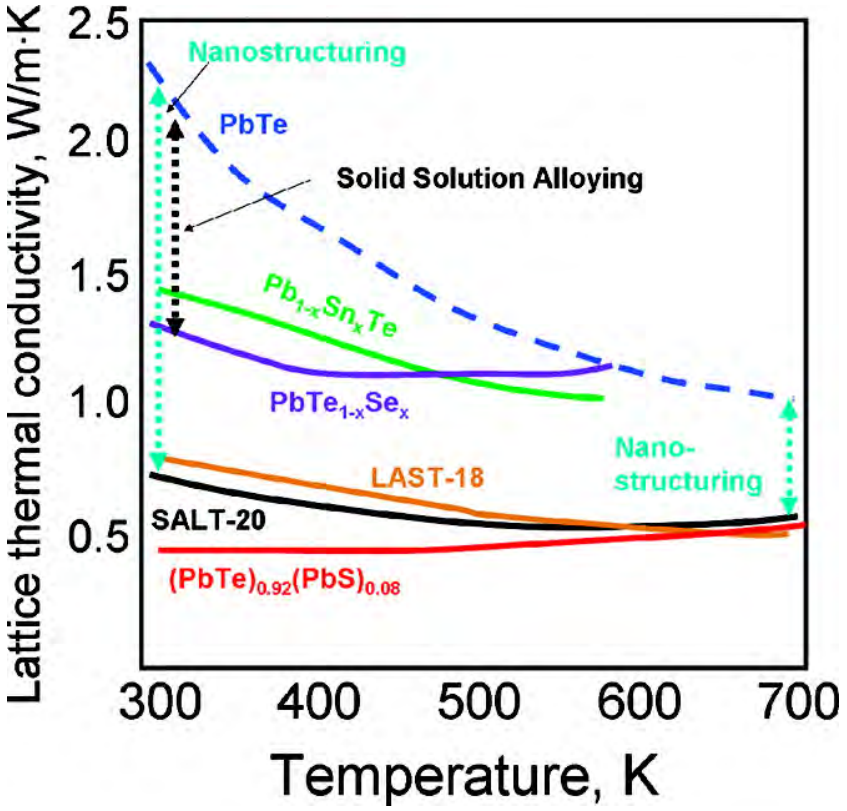

***Science* 2004**, 303, 818-821

***Nature* 2012**, 489, 414-418.

LAST-m ($Ag_{0.86}Pb_{18}SbTe_{20}$) n-type

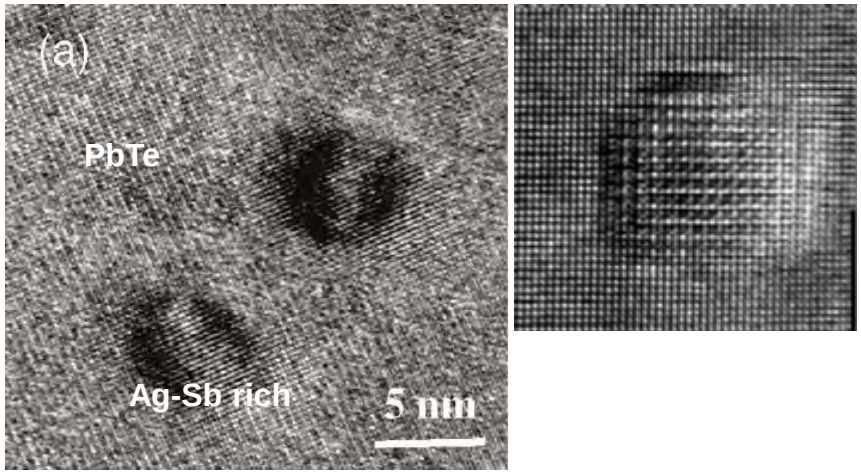

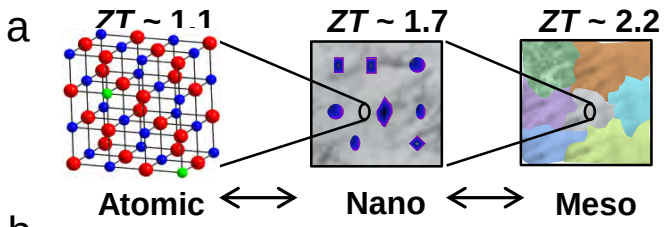

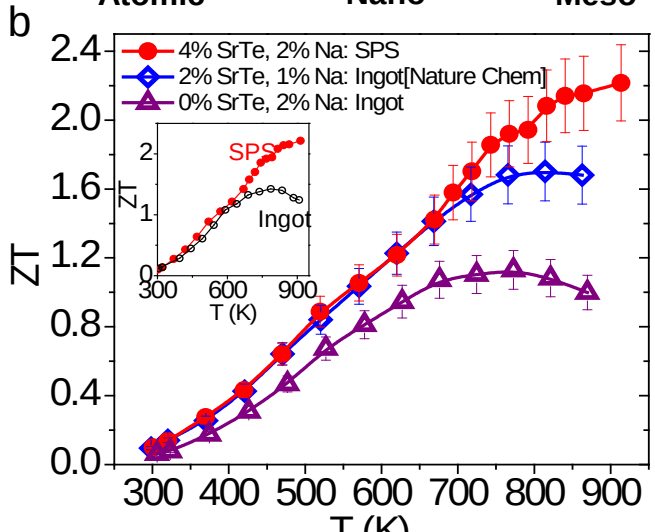

Phonon scattering mechanism in thermoelectric material

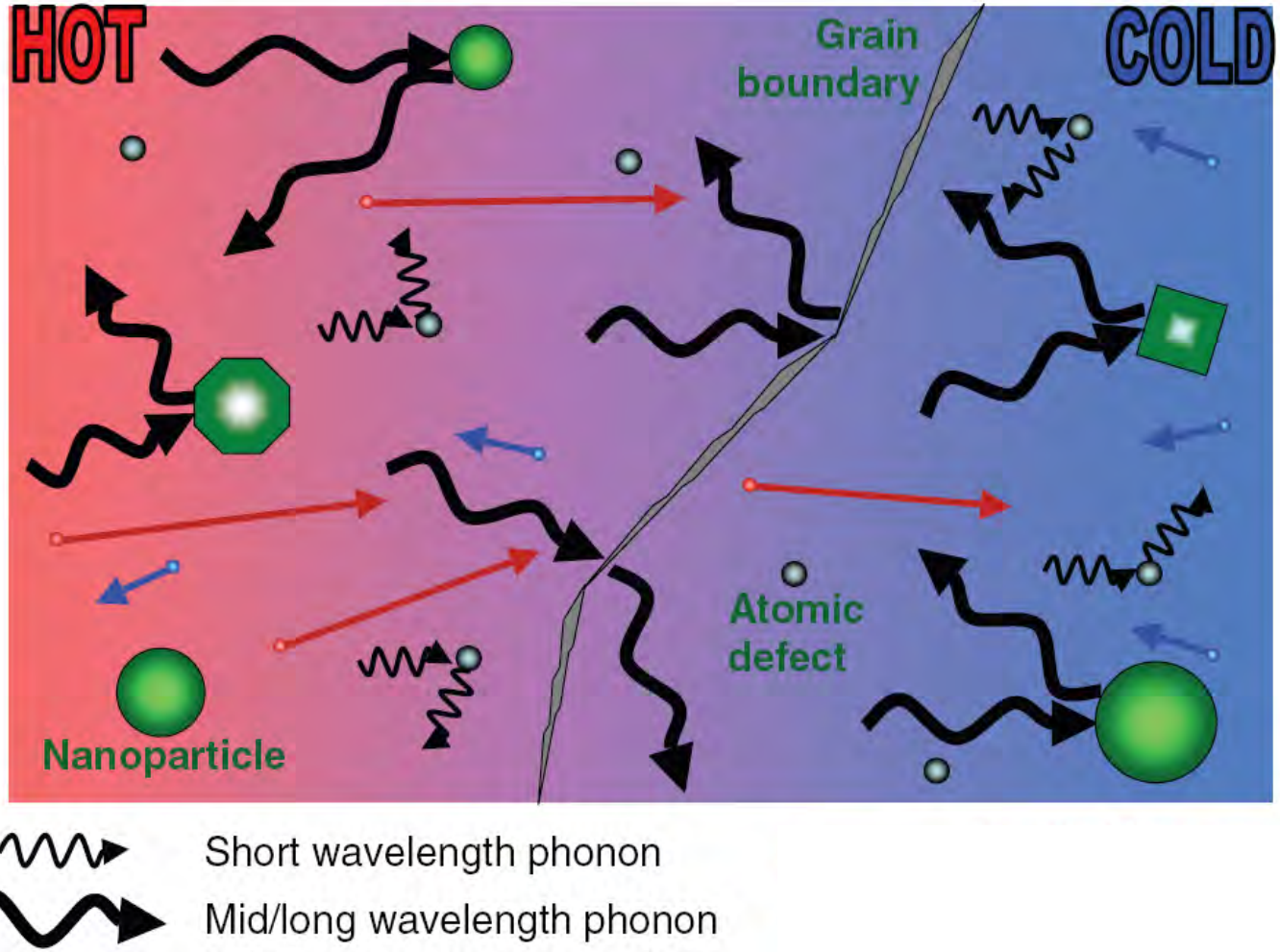

Scattering cross section = d^6/λ^4

Mid/long wavelength heat-carrying phonon heavily scattered by nanoparticles

Vines, C. J., Shakouri, A., Majumdar, A., Kanatzidis, M. G., *Adv. Mater* **2010**, 22, 3970

$$\Delta G_{mix} = \Delta H_{mix} - T\Delta S_{mix}$$

ΔH of compound formation dominates over ΔS of mixing when nanostructures forms in matrix

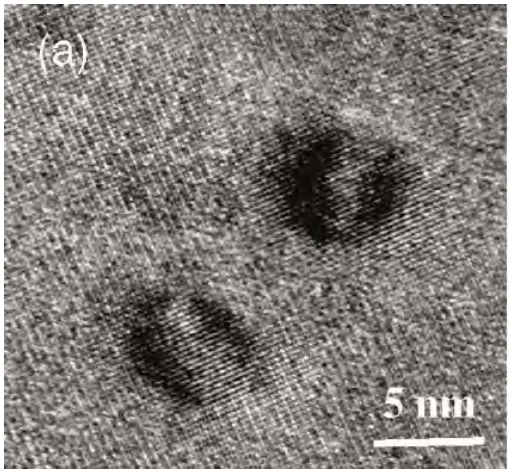

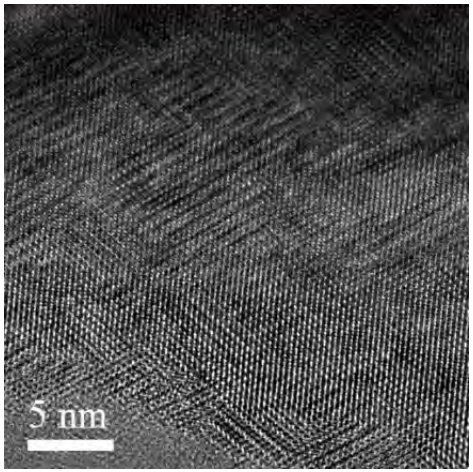

Pseudo-ternary vs. pseudo-binary

Nanostructures are good for phonon scattering, but they scatter carrier as well

$$\Delta G_{mix} = \Delta H_{mix} - T\Delta S_{mix}$$

$$\Delta G_{mix} < 0, \text{ for solid solution}$$

$$\Delta H_{mix} = H_{solid\ solution} - \Sigma H_{reactant}$$

$$\Delta S_{mix} = S_{solid\ solution} - \Sigma S_{reactant}$$

Enthalpy plays important role over entropy in binary systems (like PbTe/PbSe, GeTe/GeSe and PbTe/PbS), phase separation/nanostructuring can easily occur.

Pseudo-ternary system- Entropy of mixing dominates over enthalpy in ternary system, thus solid solution is favored. Pseudo-ternary system is rich in point defect.

GeTe-GeSe-GeS

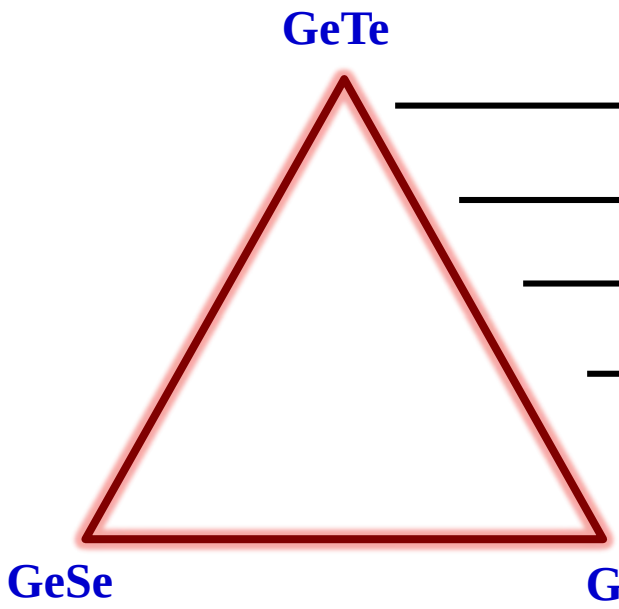

High Entropy : Atomic mixing (Solid Solution)

High Degree of Disorder

Effective point defect scattering, mass fluctuations

Reduced lattice thermal conductivity

Minimal effect on electronic transport

Strategy 1: Reduction of κ_{lat} by alloying of GeTe with GeSe and GeS .

Strategy 2: Further decrease in κ_{lat} by Sb doping in $(GeTe)_{1-2x}(GeSe)_x(GeS)_x$ and by Spark Plasma Sintering.

M. Samanta and K. Biswas, ***J. Am. Chem. Soc.*** 2017, 139, 9382

Manisha Samanta

Extended Solid Solution: $(GeTe)_{1-2x}(GeSe)_x(GeS)_x$

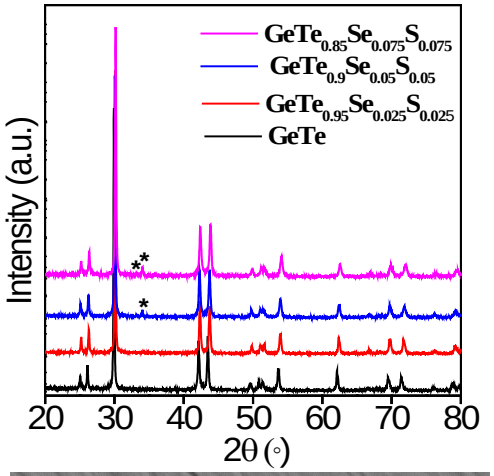

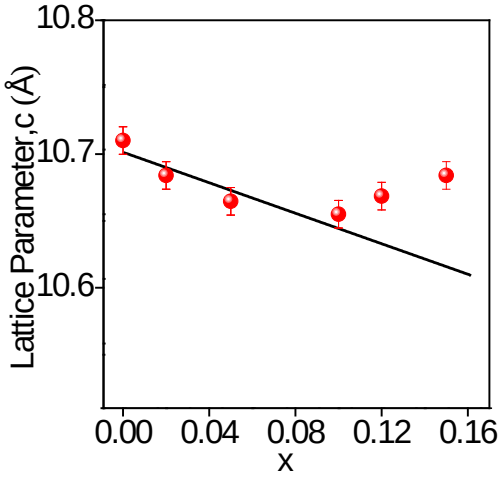

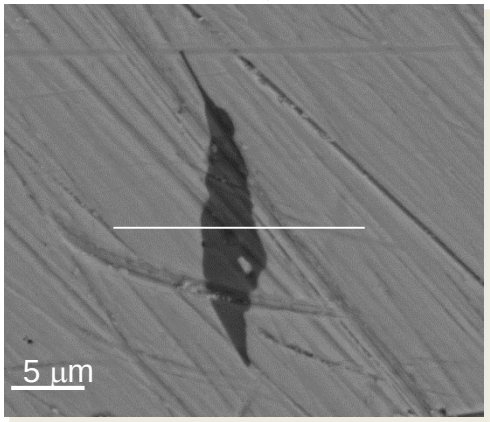

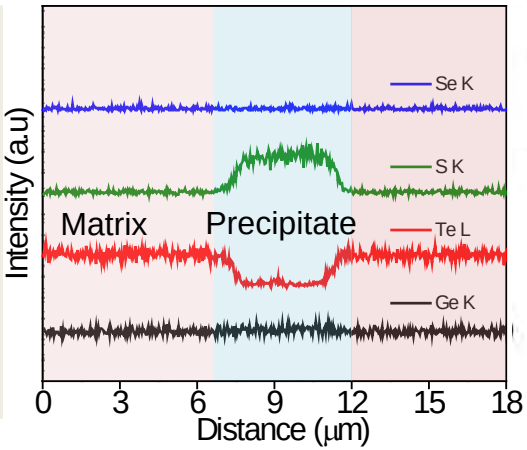

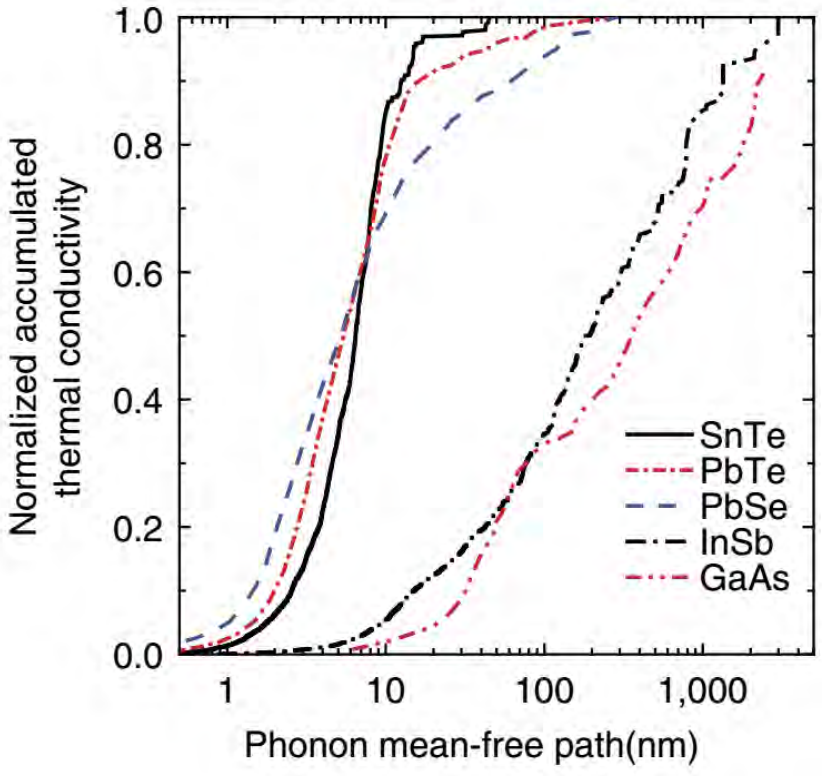

Phonons with mean free paths smaller than 10 nm comprise ~90% of the κ_{lat} for IV-VI metal tellurides. (Lee, S.; Esfarjani, K.; Luo, T.; Zhou, J.; Tian, Z.; Chen, G. *Nat. Commun.* **2014**, 5, 3525.)

Thermal conductivity: Point defect scattering

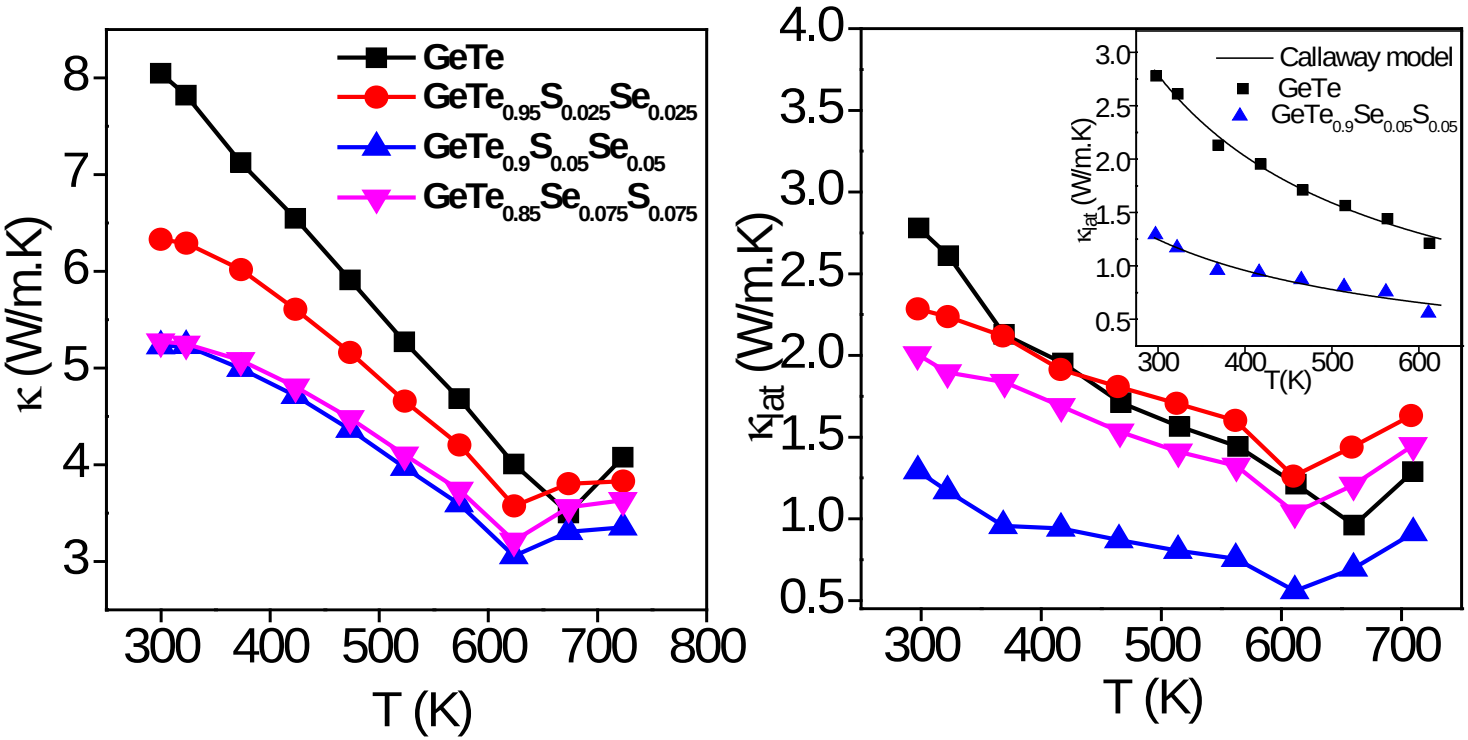

Callaway Model:

$$k_{lat} = \frac{k_B}{2v\pi^2}\left(\frac{2\pi k_B T}{h}\right)^3 \int_0^{\frac{\theta_D}{T}} \frac{\tau_C(x,T)x^4e^x}{(e^x-1)^2}dx$$

Sample	A [10^{-42} s^3]	B [10^{-17} $s\,K^{-1}$]
GeTe	1.002	1.18
$GeTe_{0.9}Se_{0.05}S_{0.05}$	13.9	2.03

$$\tau_C^{-1} = \tau_B^{-1} + \tau_{PD}^{-1} + \tau_U^{-1} + \tau_{ep}^{-1} = \frac{v}{L} + A\omega^4 + B\omega^2 T exp\left(-\frac{\theta_D}{3T}\right) + C\omega^2$$

Point defect phonon scattering dominates in $GeTe_{0.9}Se_{0.05}S_{0.05}$

Electrical Transport Properties of Sb doped $GeTe_{0.9}Se_{0.05}S_{0.05}$

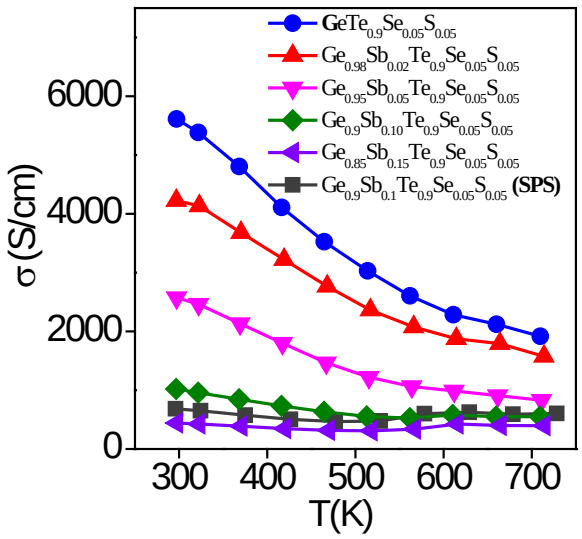

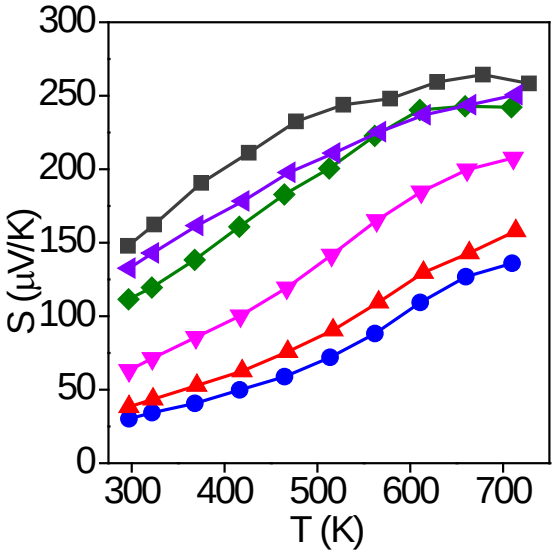

Sample	Carrier concentration (p) $\times 10^{20}/cm^3$
$Ge_{0.98}Sb_{0.02}Te_{0.9}Se_{0.05}S_{0.05}$	5.18
$Ge_{0.95}Sb_{0.05}Te_{0.9}Se_{0.05}S_{0.05}$	2.39
$Ge_{0.90}Sb_{0.1}Te_{0.9}Se_{0.05}S_{0.05}$	1.16
$Ge_{0.90}Sb_{0.1}Te_{0.9}Se_{0.05}S_{0.05}$ (SPS)	1.02
$Ge_{0.85}Sb_{0.15}Te_{0.9}Se_{0.05}S_{0.05}$	0.96

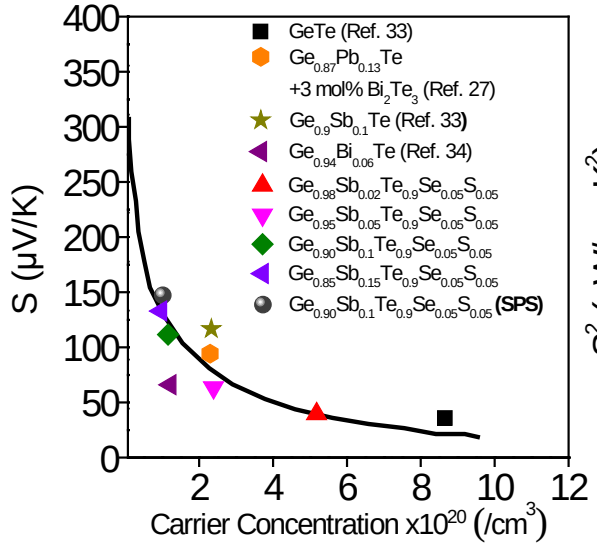

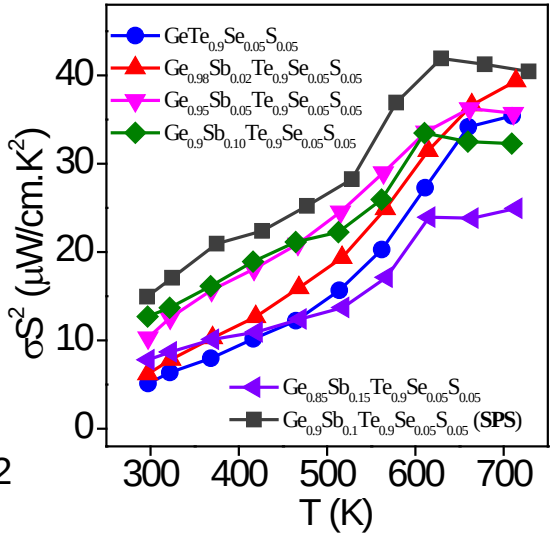

- Seebeck Coefficient increases with Sb doping
- Electrical conductivity decreases with Sb doping

M. Samanta and K. Biswas, ***J. Am. Chem. Soc.*** 2017, 139, 9382

Low lattice thermal Conductivity in $(GeTe)_{1-2x}(GeSe)_x(GeS)_x$

Pseudo-ternary vs. pseudo-binary

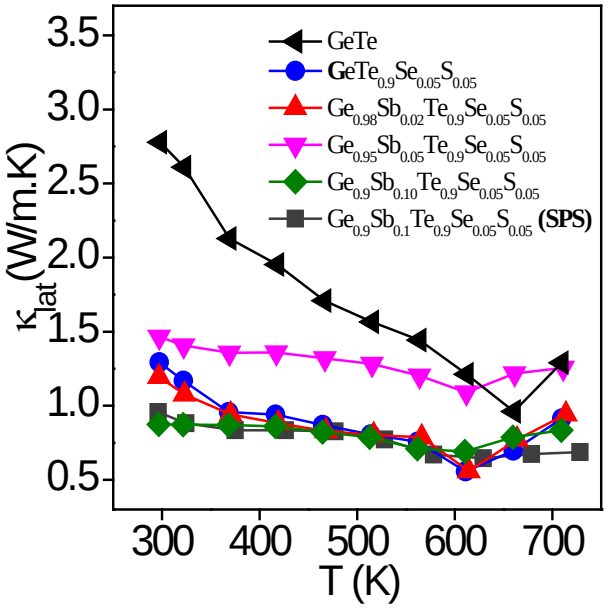

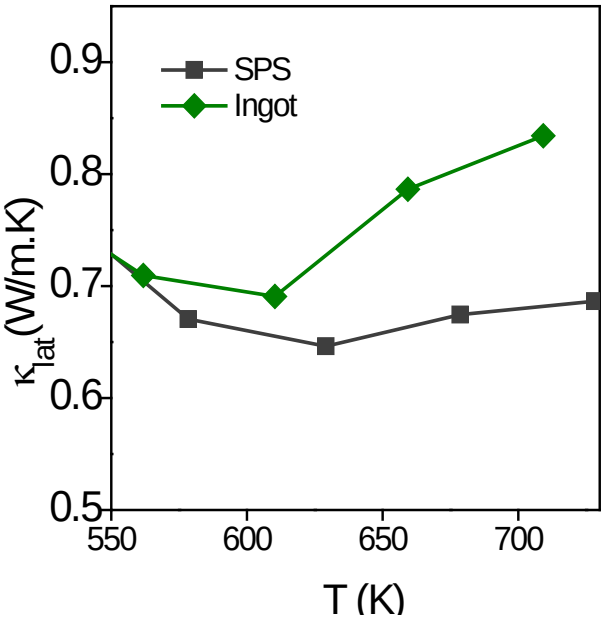

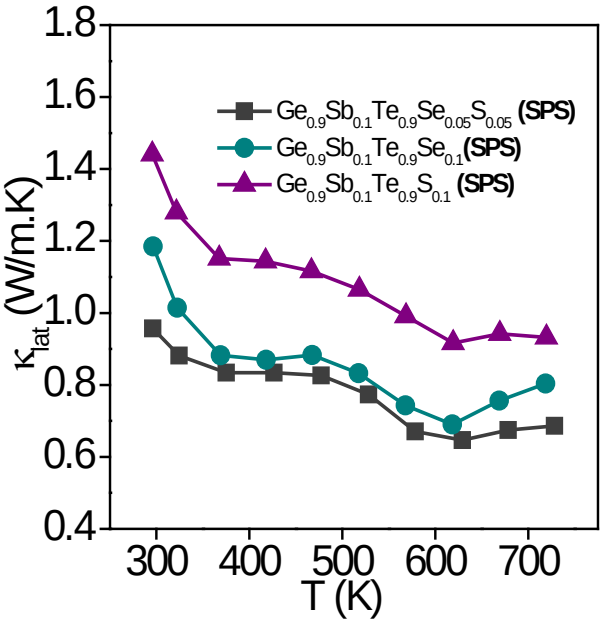

- Low k_{lat} ~ 0.7 W/mK is achieved in $Ge_{0.9}Sb_{0.1}Te_{0.9}Se_{0.05}S_{0.05}$ (SPS).
- GeTe-GeSe-GeS psedo ternary system shows lower k_{lat} than GeTe-GeSe and GeTe-GeS pseudo binary system.
- Phonon scattering mainly occurs due to effective point defect scattering involving a broad set of multiple types of mass fluctuations such as Ge/Sb, Te/Se, Te/S and Se/S.

ZT = 2.1 in Pb free GeTe based system

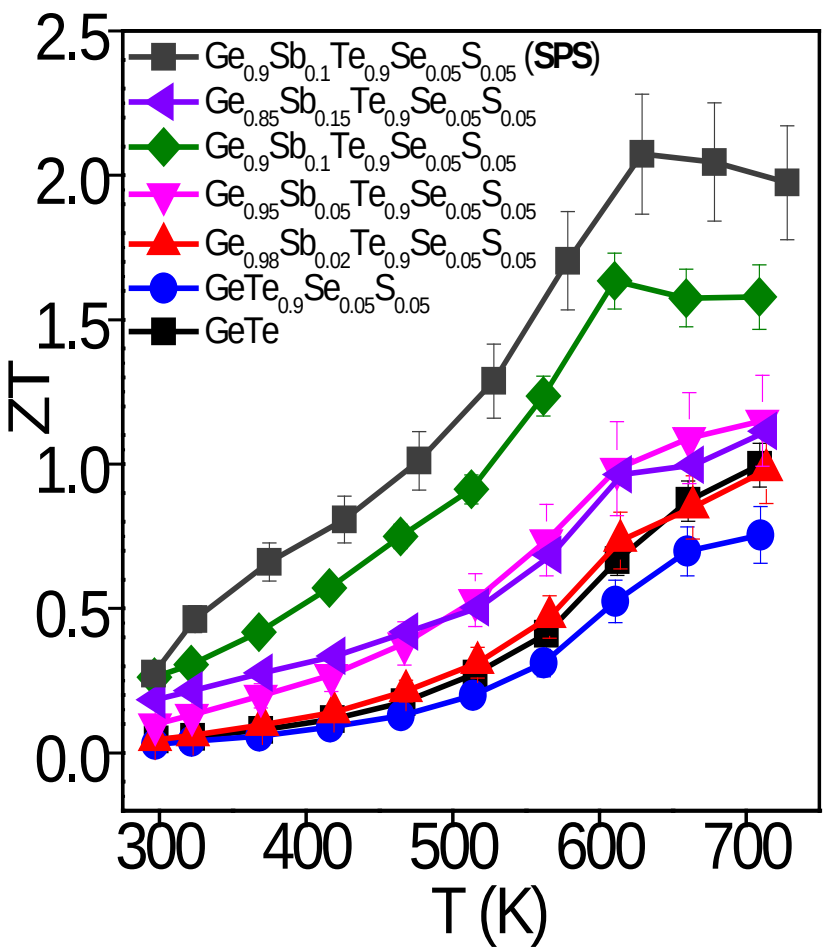

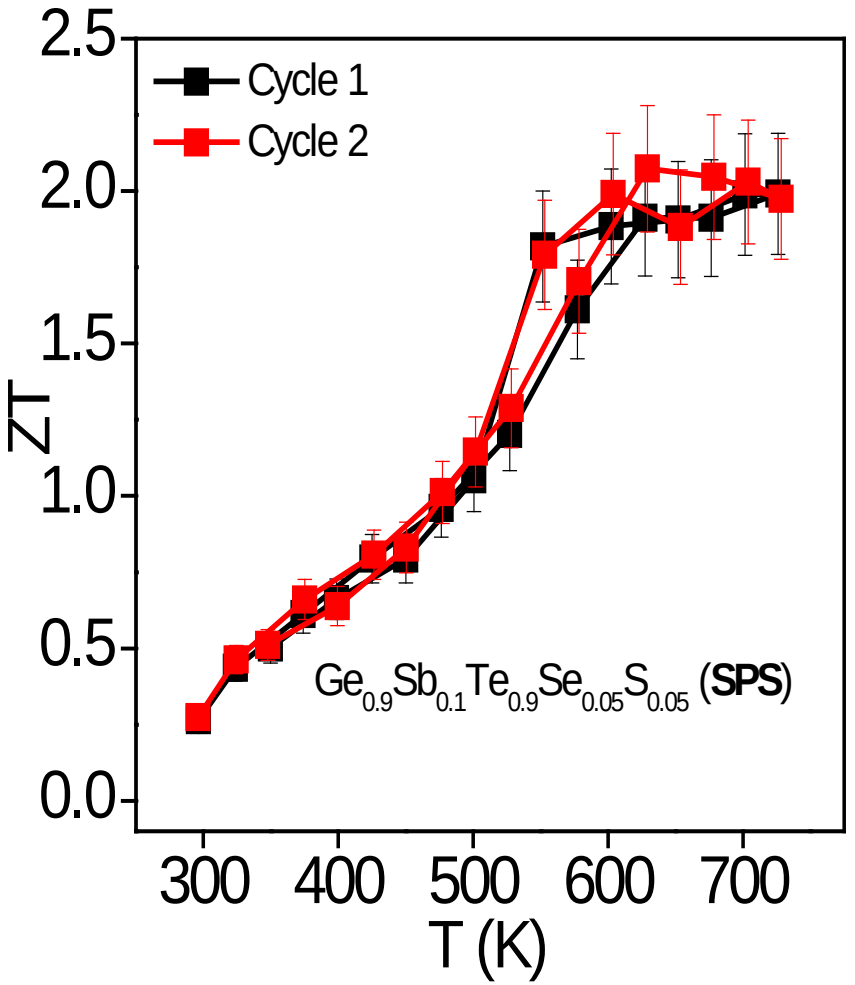

M. Samanta, K. Biswas, ***J. Am. Chem. Soc.*** 2017, 139, 9382

Extrinsic approach- Introduction of point defects, nanoprecipitates and grain boundaries.

They scatters the phonons heavily, but scatters the electrons/holes as well.

Intrinsic low thermal conductivity is of practical interest due to its robustness against grain size, temperature range and other structural variations.

Ultralow Thermal Conductivity in Zintl Type $TlInTe_2$

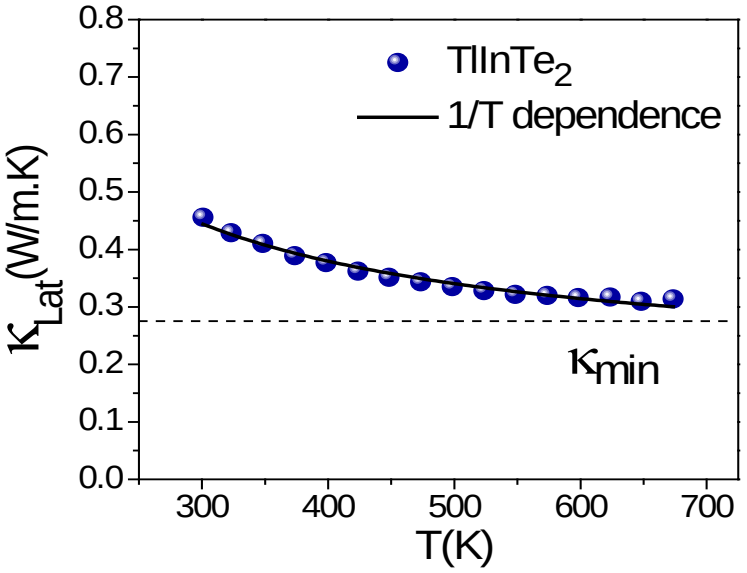

Slack's formalism (at high T)

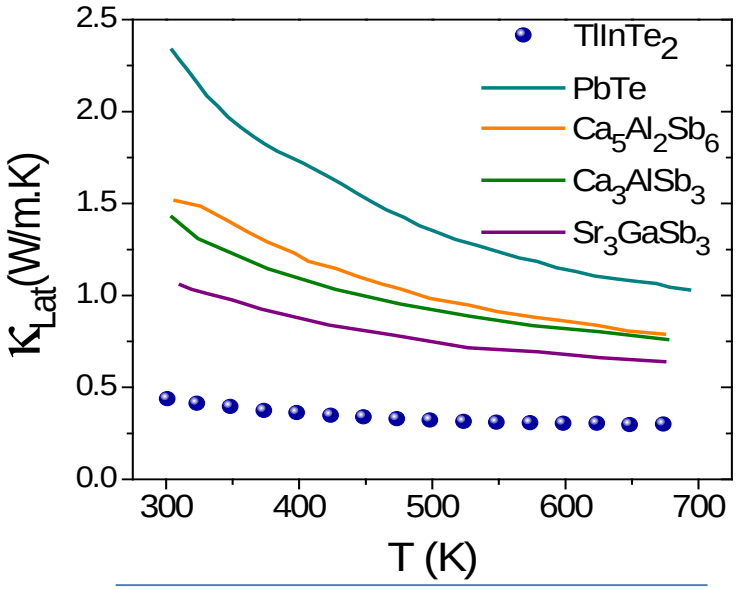

Cahill's minimum thermal conductivity

$$\kappa_{Lat} = \frac{A\bar{M}\theta^3\delta}{\gamma^2 n^{2/3}\ T}$$

$$\kappa_{min} = \left(\frac{\pi}{6}\right)^{1/3} k_B n_a^{2/3} \sum_i v_i \left(\frac{T}{\theta_i}\right)^2 \int_0^{\theta_i/T} \frac{x^3 e^x}{(e^x-1)^2}\, dx$$

- 1/T dependence of lattice thermal conductivity suggests dominant anharmonic Umklapp phonon scattering.
- Ultralow lattice thermal conductivity approaching theoretical amorphous-limit (κ_{min}) at high temperatures.

M. K. Jana, K. Pal, A. Warankar, P. Mandal, U. V. Waghmare, K. Biswas, ***J. Am. Chem. Soc***, 2017, 139, 4350

Intrinsic Rattler-Induced Low Thermal Conductivity in Zintl Type $TlInTe_2$

Crystal structure of $TlInTe_2$

I 4/m c m - tetragonal

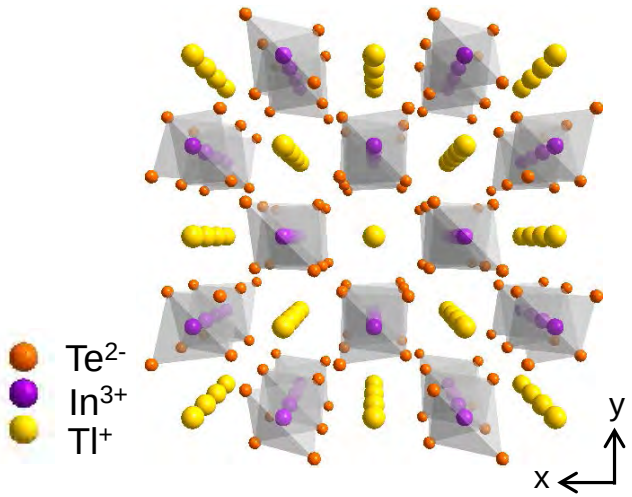

Covalent substructure

Ionic substructure

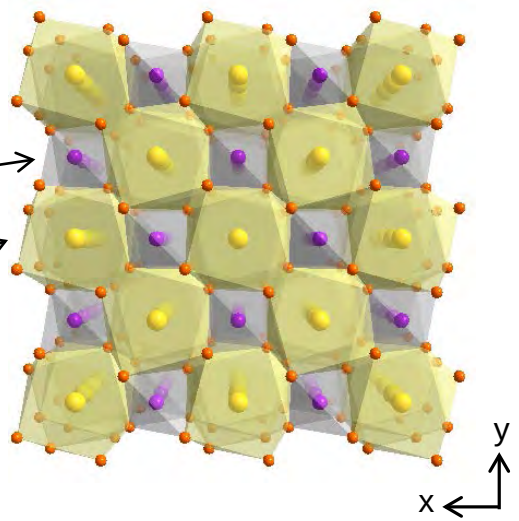

Intrinsic bonding hierarchy

- Anionic and cationic substructures resembling 1D-zintl compounds
- Covalently bonded chains of ($InTe_4$) tetrahedra along the z-axis (violet)
- Each Tl^+ cation is centered in a distorted square antiprism of Te ions (Thompson cubes)
- Anionic chains are held electrostatically by chains of Tl^+ cations.

Ultralow Thermal Conductivity in Zintl Type $TlInTe_2$

Synthesis

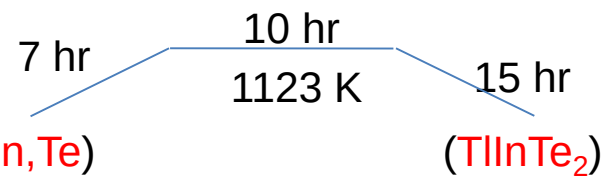

Fused quartz ampoules (10^{-5} torr)

SPS

50 MPa, 723 K,

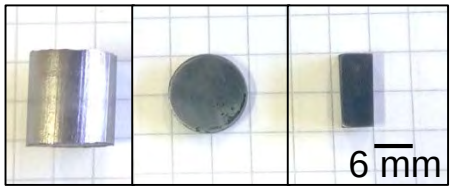

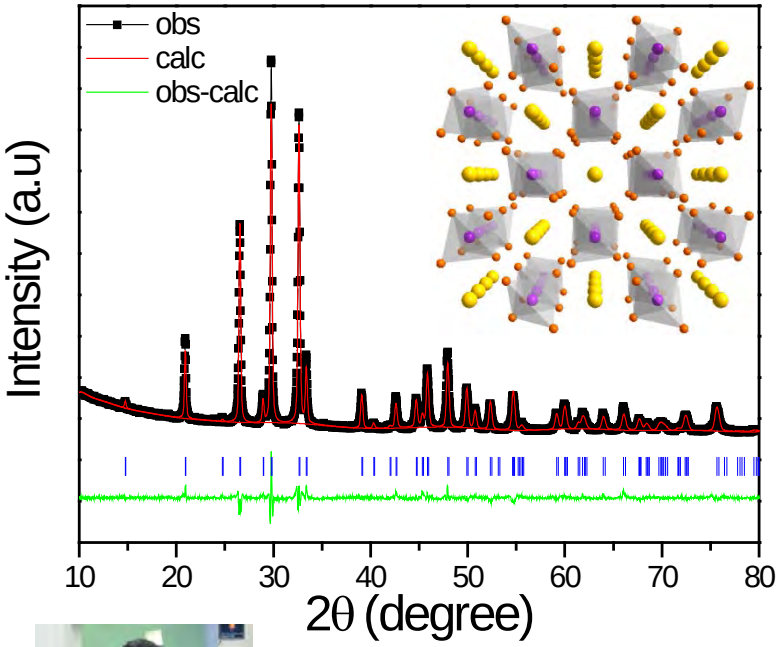

Structural parameters from Rietveld refinement						
	a	b	c	Vol (Å^3)		
I4/mcm	8.47980 (27)	8.47980 (27)	7.18894 (28)	516.94 (5)		
	x	y	z	U_{iso} (Å^2)		
In	0	0.5	0.25	0.01674		
Te	0.18098	0.68098	0	0.0235		
				U_{11}	U_{22}	U_{33}
Tl	0	0	0.25	0.02759	0.02759	0.07442

Manoj

Anisotropic, large atomic displacement parameters (ADPs) of Tl^+

Structure and bonding in $TlInTe_2$

Valence charge density

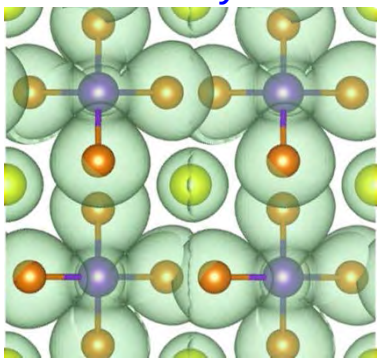

Electron localization

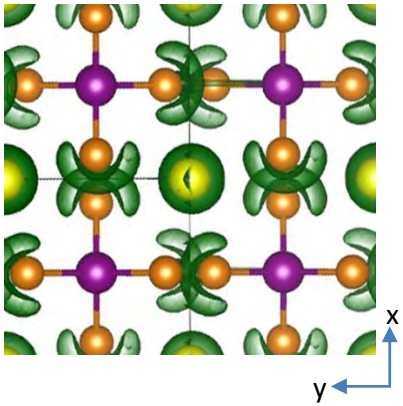

ADP ellipsoids (80% probability)

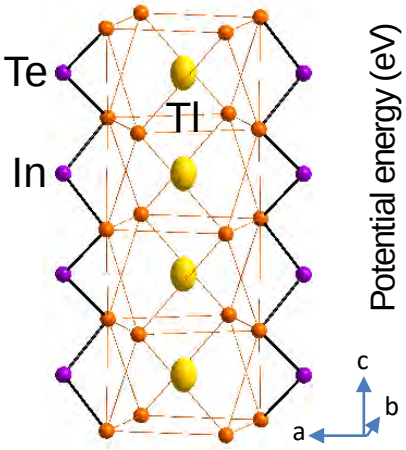

Potential energy wells

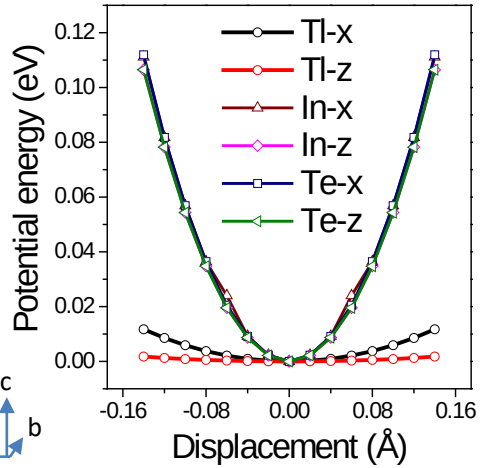

- Covalent bonding within ($InTe_4$) tetrahedron and isolated Tl^+ cations.
- Spherical charge density around Tl^+ cation → $6s^2$ lone electron pair
- Spherical lone pairs are unstable and are known to form stereochemical lobes by distorting the structure.

(e.g. *Lone-pair driven monoclinic distortion of perovskite $BiMnO_3$*)

- Steep potential wells for In and Te atoms but flat potential well for Tl atoms
- No apparent distortion in the average structure
- Consequently, phonons may be highly anharmonic

(Nielsen et al, *Energy Environ. Sci.* **2013**, *6*, 570)

Tl - intrinsic rattler

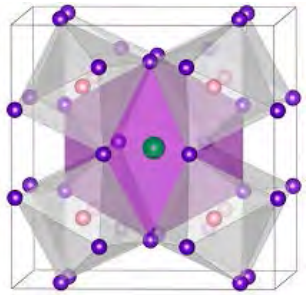

Filled-skutterudite

Low temperature heat capacity of $TlInTe_2$

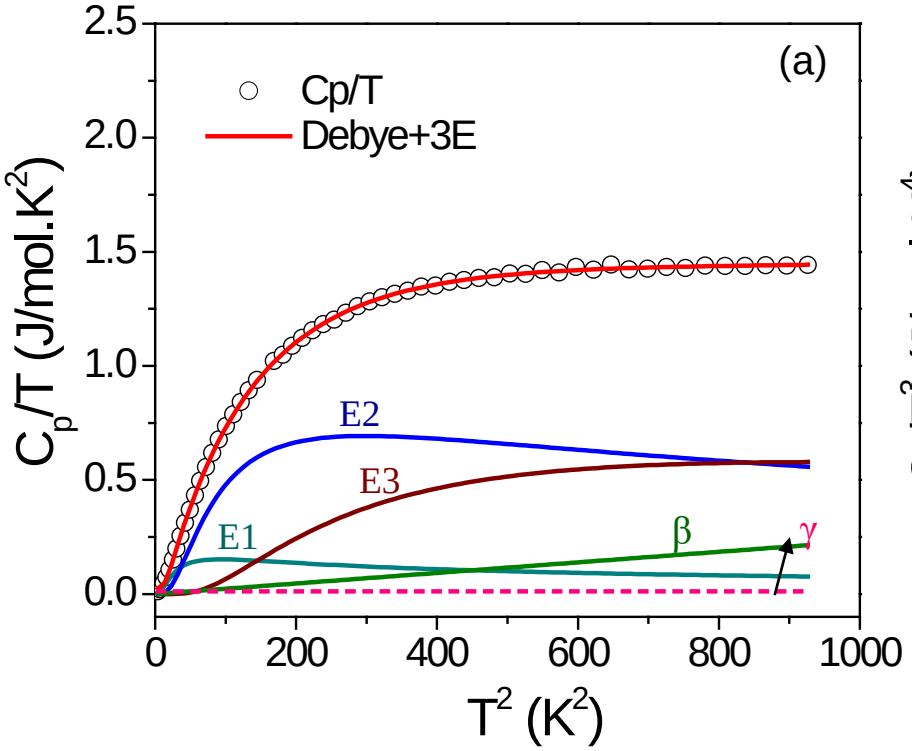

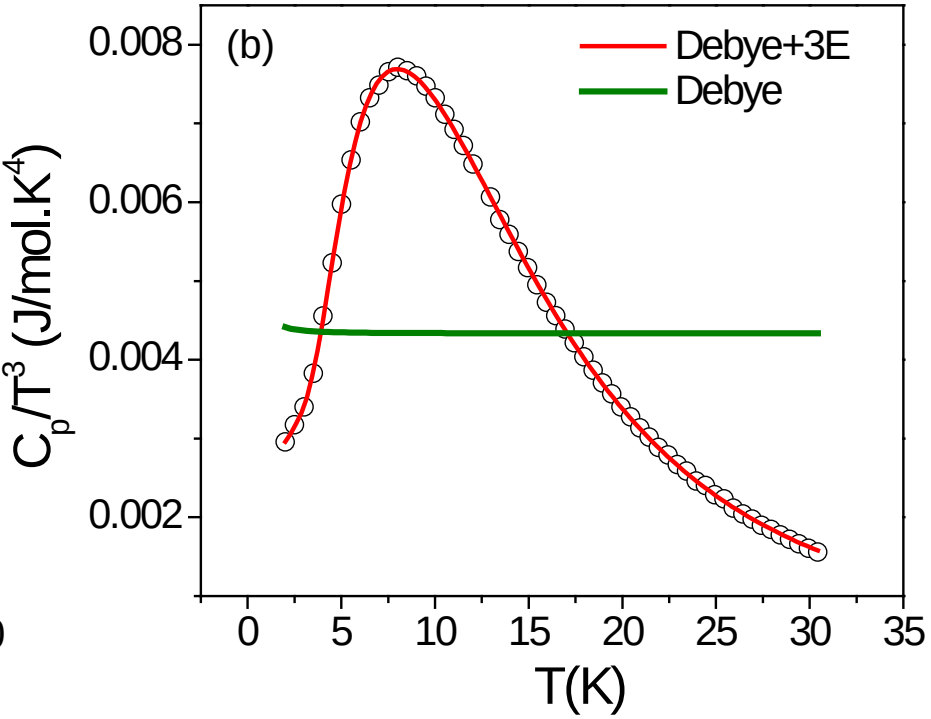

Debye-Einstein model

$$C_P/T = \gamma + \beta T^2 + \sum_i \left(A_i (\Theta_{E_i})^2 \cdot (T^2)^{-\frac{3}{2}} \cdot \frac{e^{\frac{\Theta_{E_i}}{T}}}{\left(e^{\frac{\Theta_{E_i}}{T}} - 1\right)^2} \right)$$

- Low temperature specific heat capacity shows the contribution of Einstein oscillators with frequencies of about 17, 30 and 55 cm^{-1}
- The low-energy Einstein modes are related to low-frequency, localized optic-like vibrations. The latter can scatter the heat-carrying acoustic phonons and suppress thermal conductivity significantly.

M. K. Jana, K. Pal, A. Warankar, P. Mandal, U. V. Waghmare, K. Biswas, ***J. Am. Chem. Soc***, 2017, 139, 4350

THz spectra of $TlInTe_2$

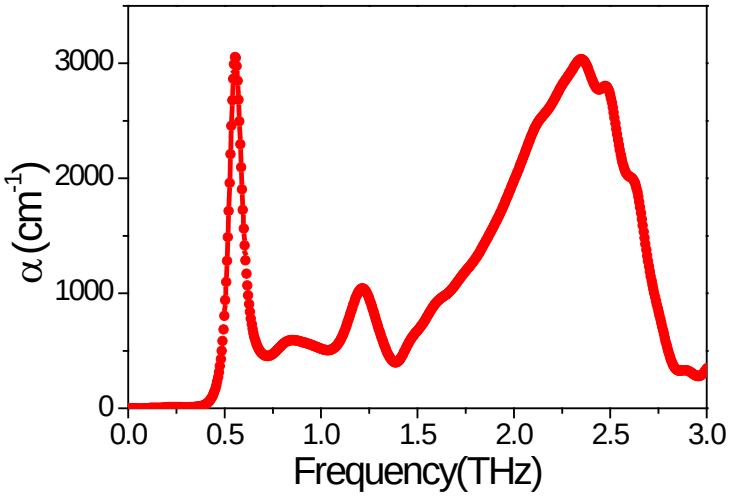

Pankaj Mandal, IISER, Pune

Phonon dispersion of $TlInTe_2$

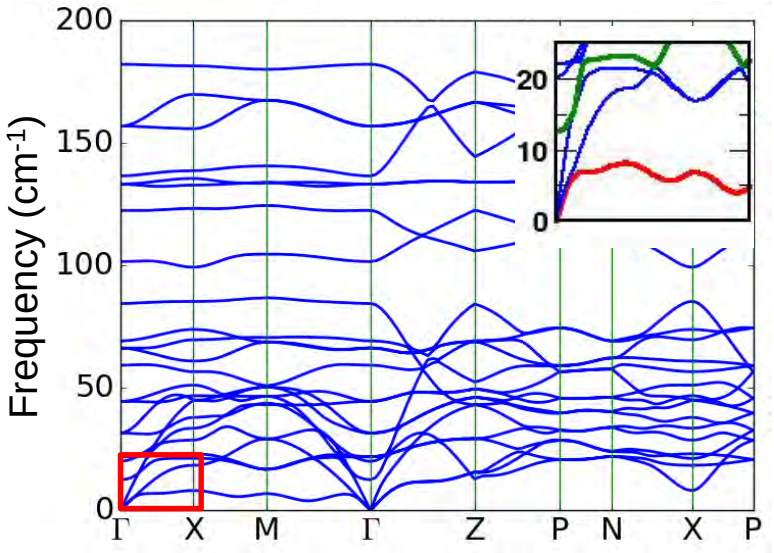

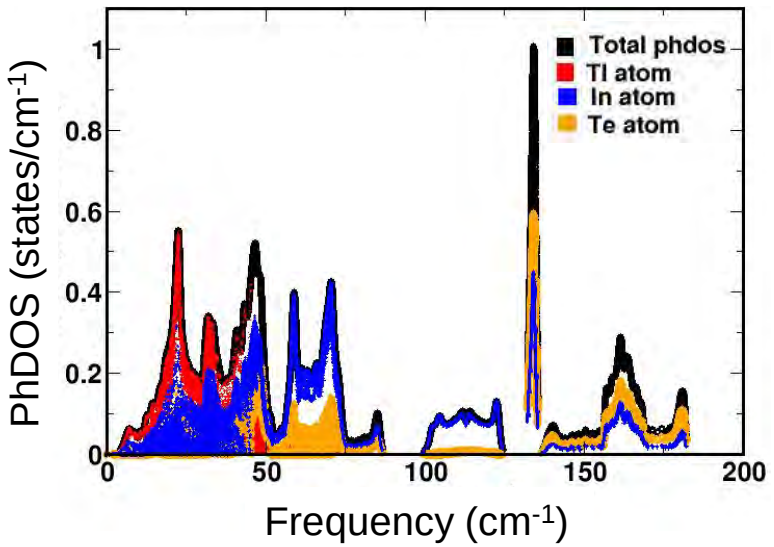

Umesh Waghmare, JNCASR, Bangalore

Soft Phonon Modes Leading to Ultralow Thermal Conductivity and High Thermoelectric Performance in AgCuTe

Crystal Structure of AgCuTe

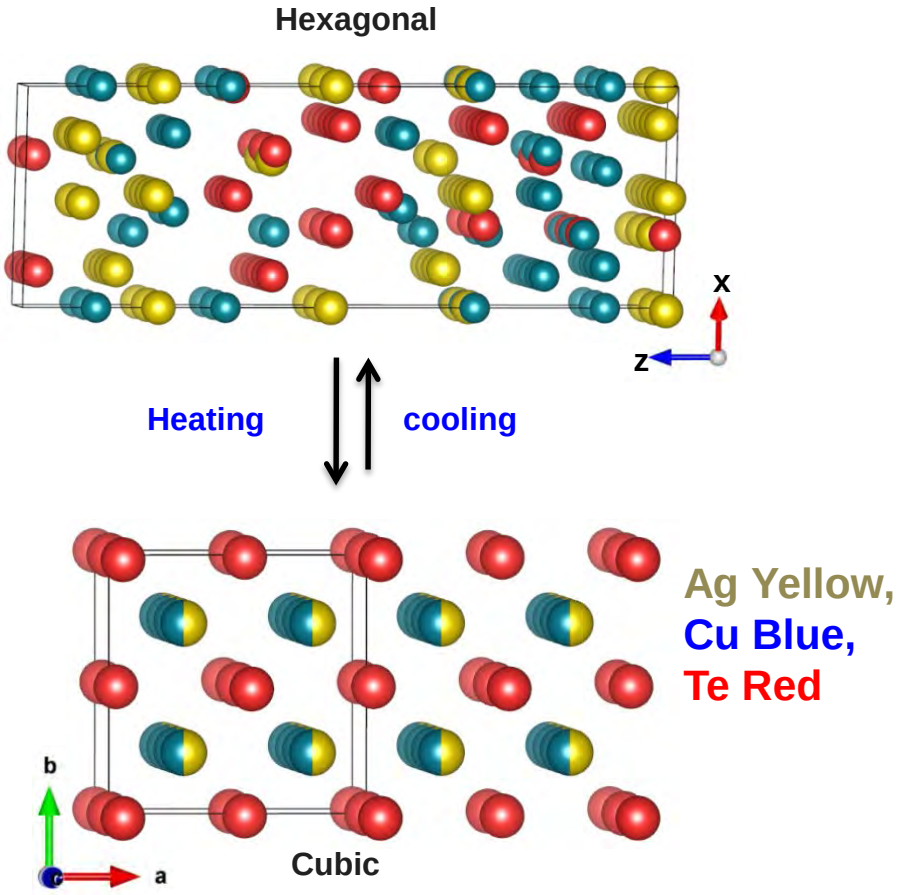

Ag Yellow,
Cu Blue,
Te Red

synchrotron experiments at the Indian Beamline, PF, KEK, Japan

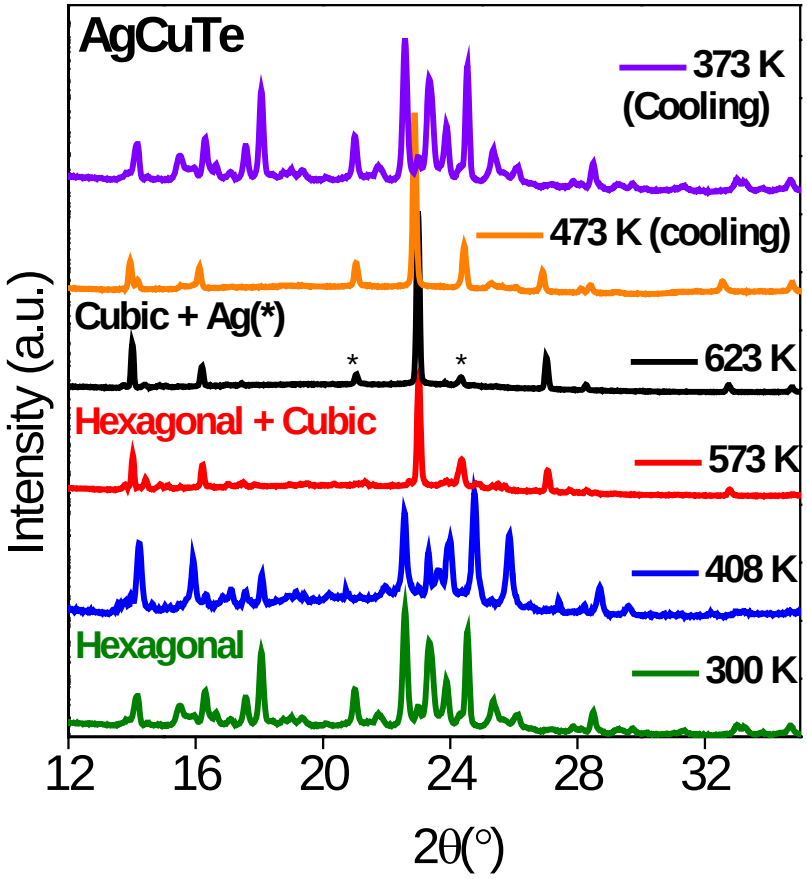

S. Roychowdhury, M. K. Jana, J. Pan, S. N. Guin, D. Sanyal, U. V. Waghmare, K. Biswas, ***Angew. Chem. Int. Ed.*** 2018, 57, 4043

Positron annihilation spectroscopy: Role of Ag vacancy

Positron annihilation Lifetime Spectrum

Doppler broadened spectrum

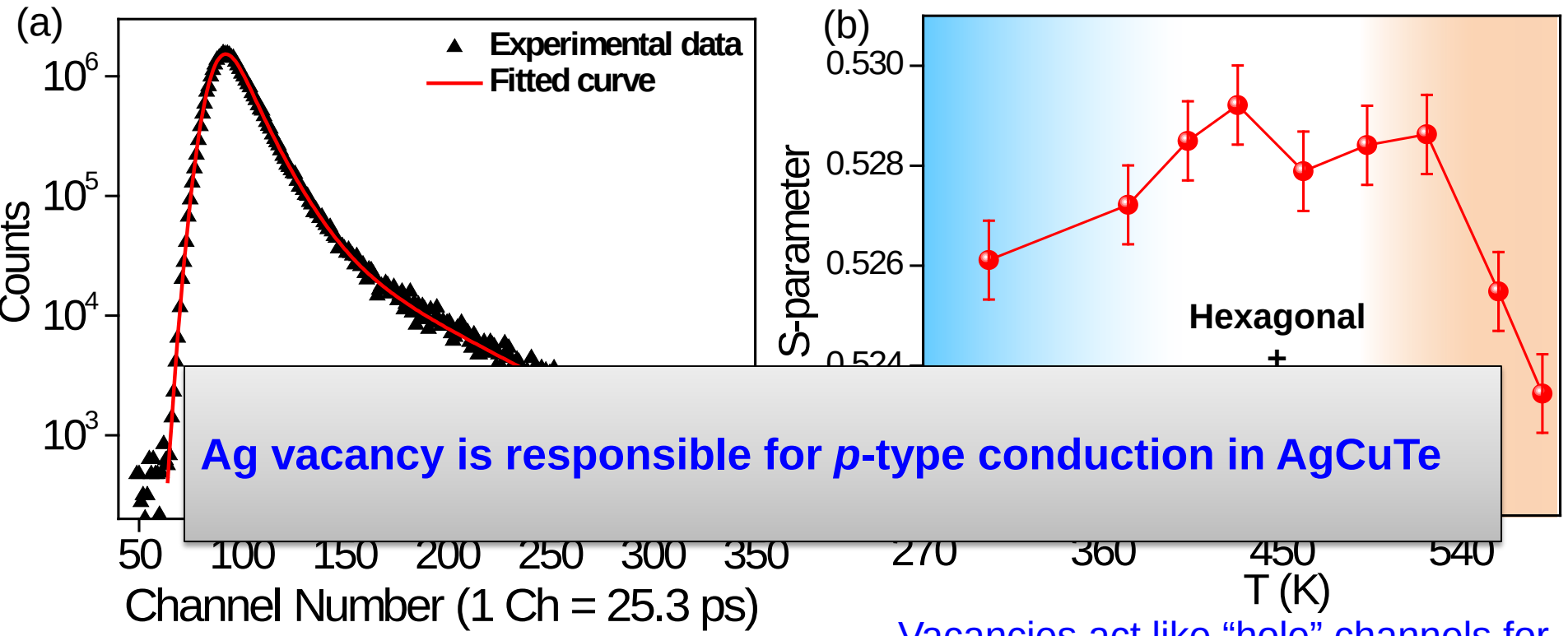

Ag vacancy is responsible for *p*-type conduction in AgCuTe

Vacancies act like “hole” channels for superionic conduction of cations

Lifetime component: 304±3 ps **:**
Ag Vacancy

The S-parameter represents the fraction of positrons annihilating with the low-momentum valence electrons with respect to the total number of positrons annihilated

Ultralow thermal conductivity

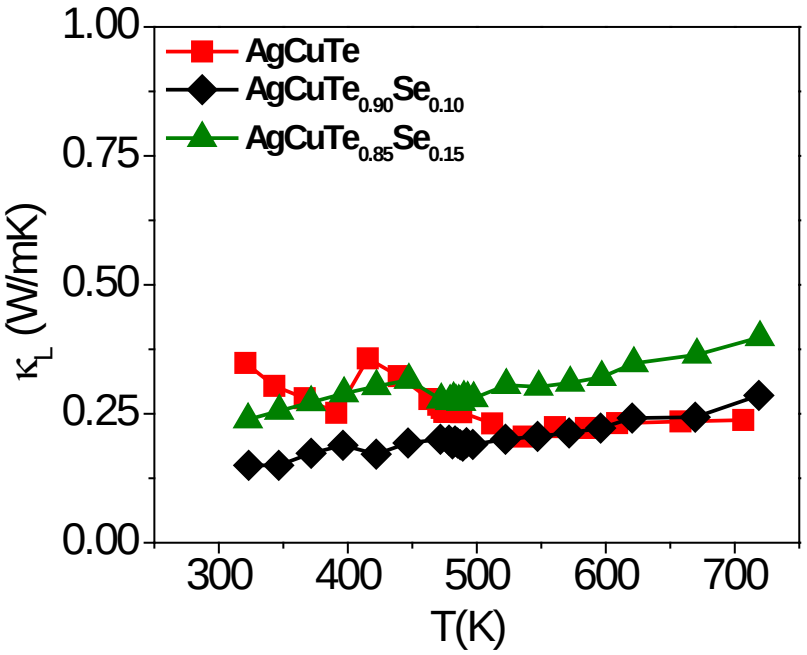

Subhajit Roychowdhury

Low-T Heat Capacity for AgCuTe

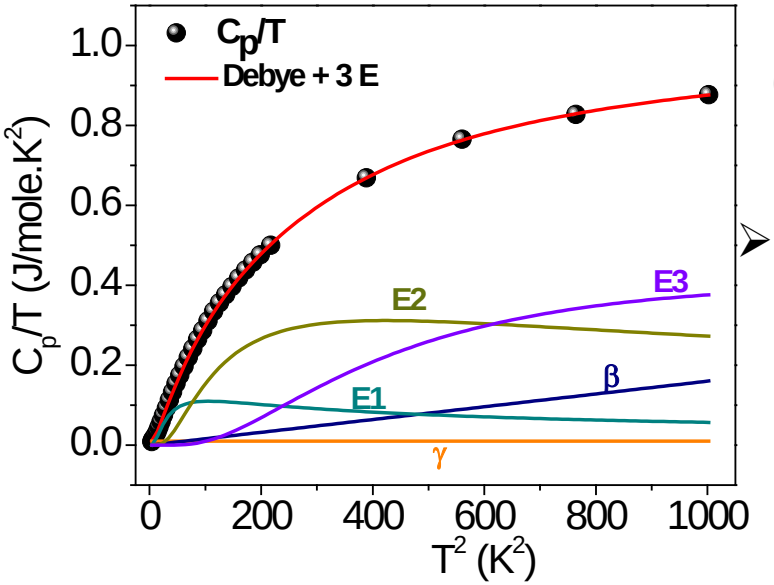

Debye-Einstein model

$$C_P/T = \gamma + \beta T^2 + \sum_i \left(A_i(\Theta_{E_i})^2 \cdot (T^2)^{-\frac{3}{2}} \cdot \frac{e^{\frac{\Theta_{E_i}}{T}}}{\left(e^{\frac{\Theta_{E_i}}{T}} - 1\right)^2} \right)$$

- The low-energy Einstein modes (26, 52 and 103 cm^{-1}) are related to low-frequency, localized optic-like vibrations which can scatter the heat-carrying acoustic phonons and suppress thermal conductivity significantly.

Phonon Density of States

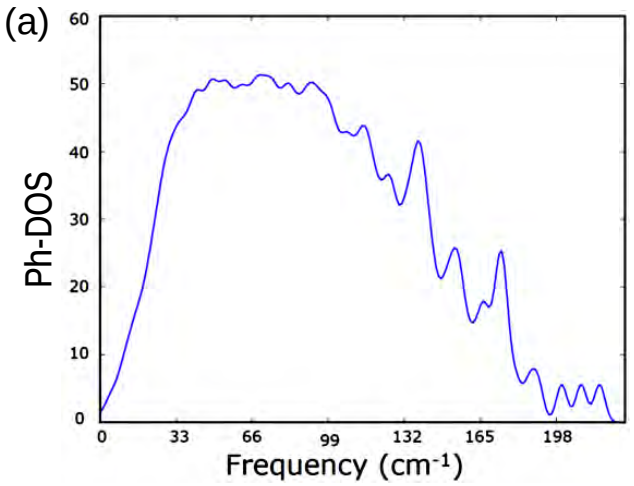

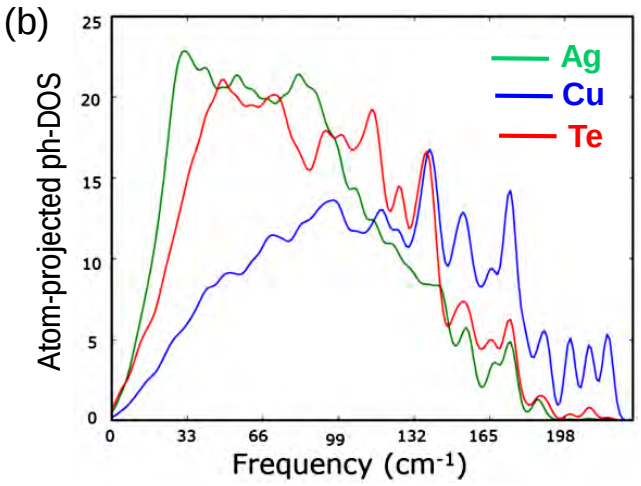

Ph-DOS of the hexagonal phase reveals unusually many "soft' vibrational modes with frequencies lower than 50 cm^{-1}

Dominant contributions from Ag ionic displacements

(c)

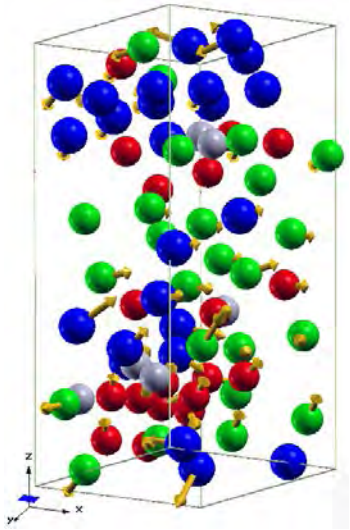

Mode 1 (5.14 cm^{-1})

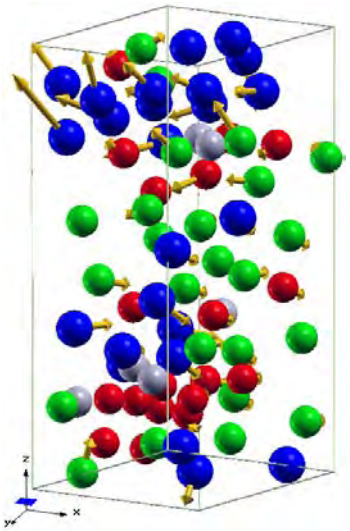

Mode 2 (9.45 cm^{-1})

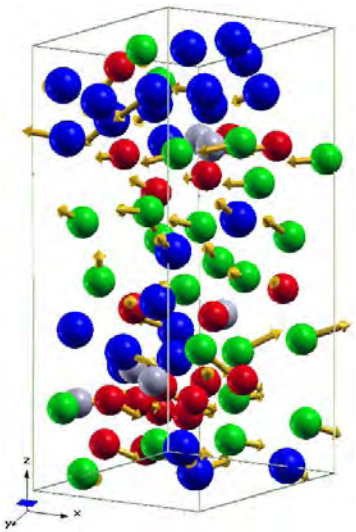

Mode 3 (12.65 cm^{-1})

Optical-acoustic phonon coupling

Ag blue, Cu red, Te green

In collaboration with Prof. Umesh V. Waghmare

Electronic transport properties of AgCuTe

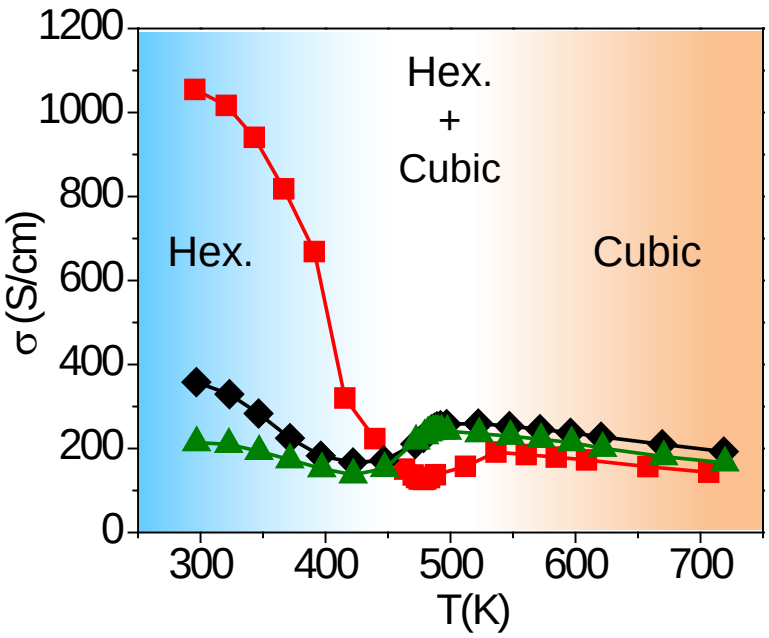

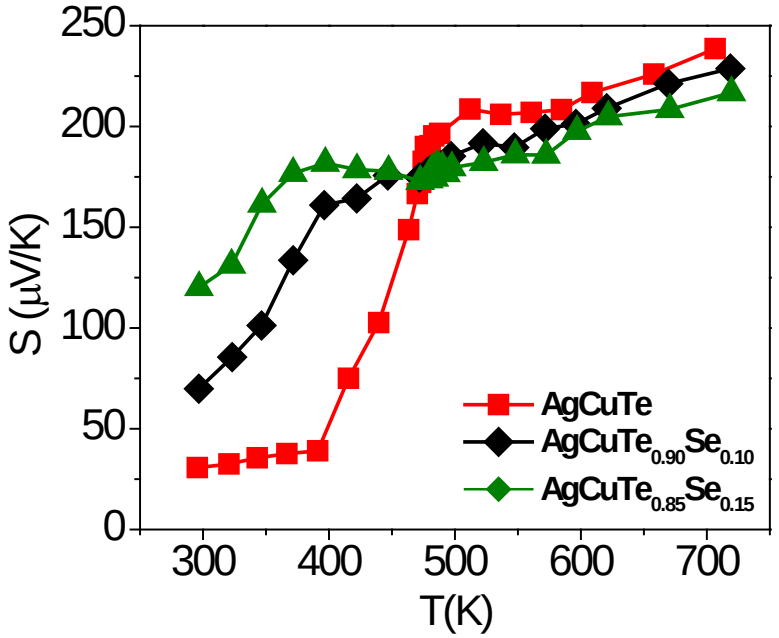

Sample	Carrier Concentration (cm^{-3})	Mobility (cm^2/Vs)
AgCuTe	9.74 X 10^{18}	676
$AgCuTe_{0.90}Se_{0.10}$	6.24 X 10^{18}	361
$AgCuTe_{0.85}Se_{0.15}$	4.53 X 10^{18}	297

Electronic structure

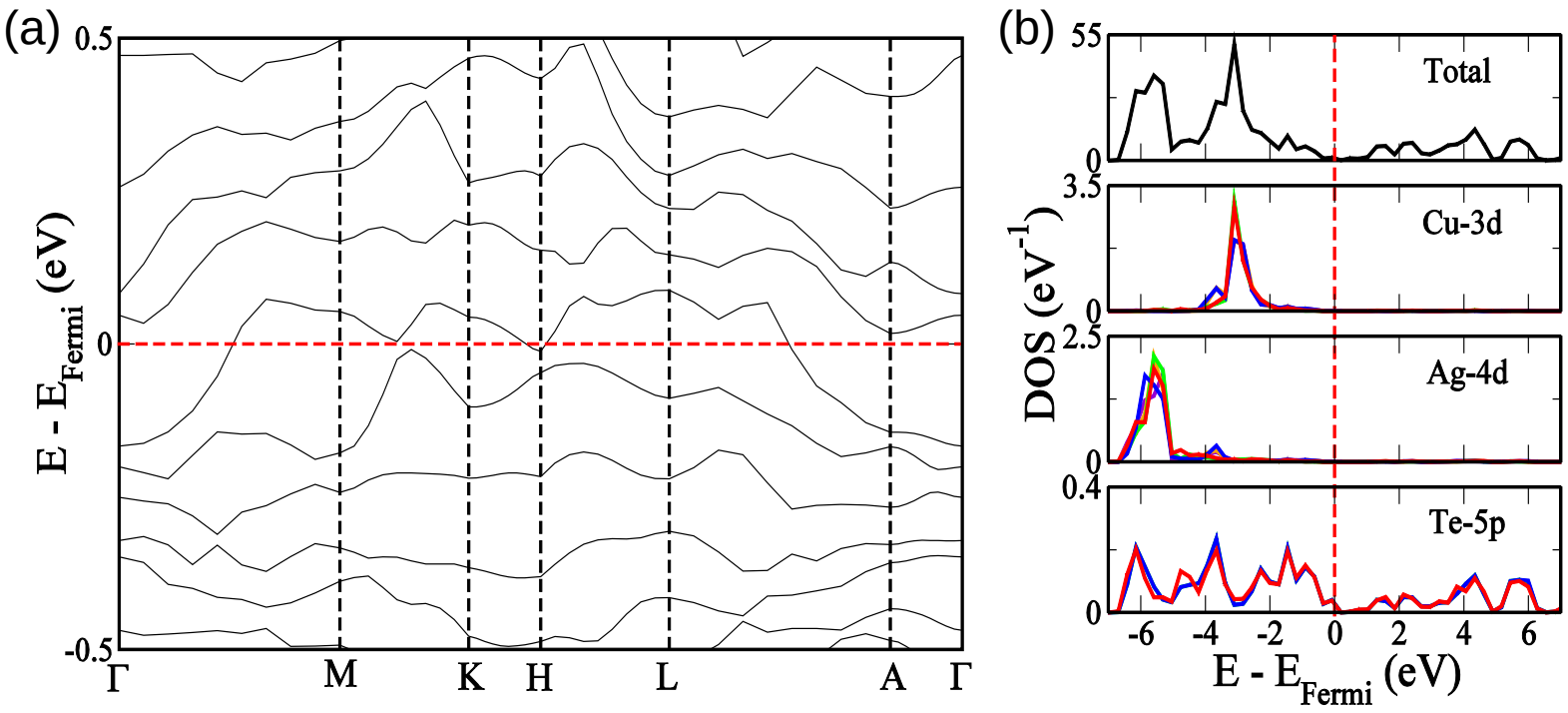

Hexagonal AgCuTe is semimetallic

Thermoelectric Figure of Merit

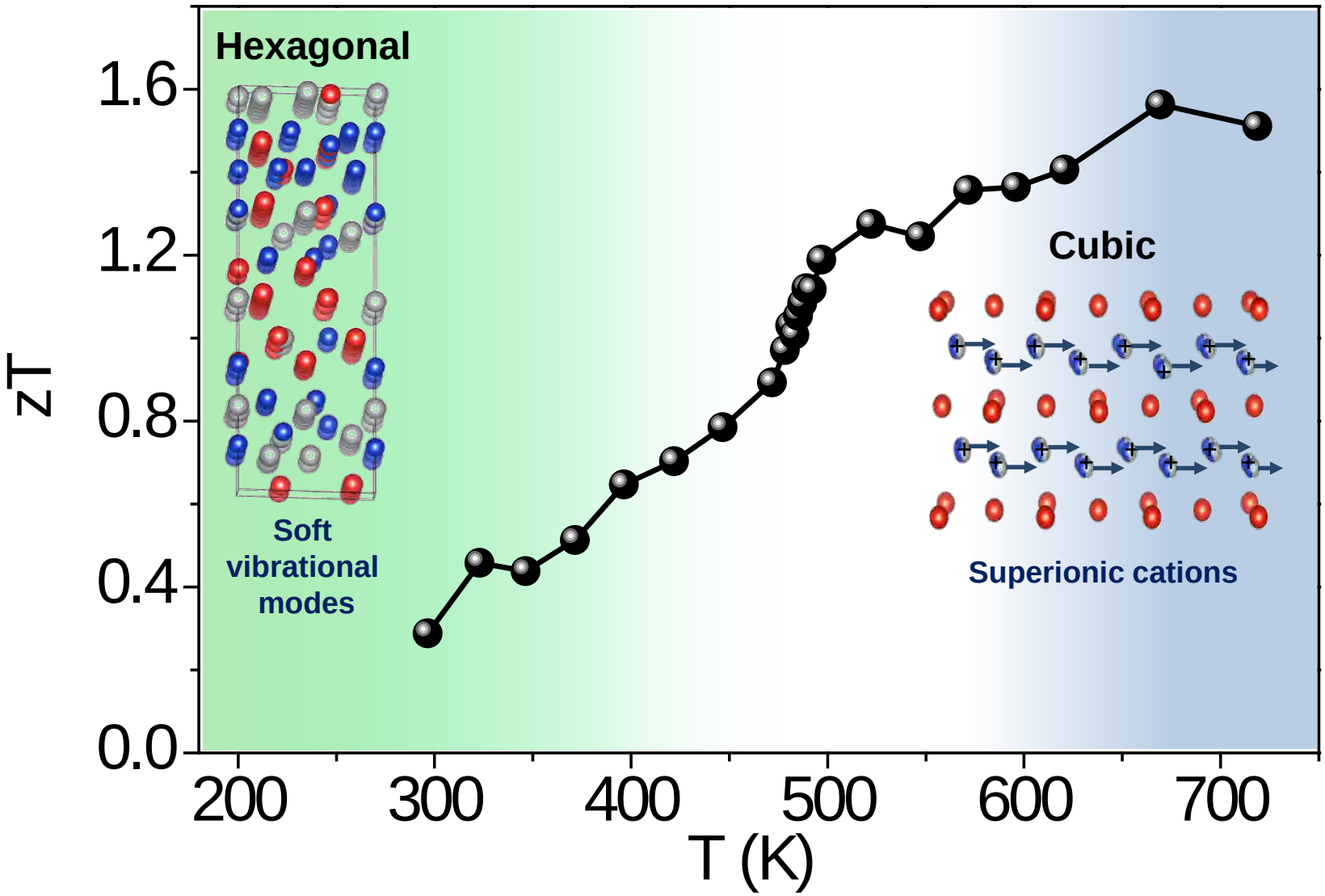

VIP Thermoelectrics Very Important Paper

International Edition: DOI: 10.1002/anie.201801491
German Edition: DOI: 10.1002/ange.201801491

Soft Phonon Modes Leading to Ultralow Thermal Conductivity and High Thermoelectric Performance in AgCuTe

*Subhajit Roychowdhury, Manoj K. Jana, Jaysree Pan, Satya N. Guin, Dirtha Sanyal, Umesh V. Waghmare, and Kanishka Biswas**

Media Coverage

THE HINDU
INDIA'S NATIONAL NEWSPAPER SINCE 1878

"JNCASR's novel material to convert waste heat into electricity",
(March 03, 2018).

The Indian EXPRESS

"No side effects: Finding compound that conducts electricity, not heat",
(March 12, 2018).

The Telegraph

"New material raises hope of turning waste heat into power",
(March 04, 2018).

THE BETTER INDIA

"Can Waste Heat Generate Electricity? These Bengaluru Researchers Say Yes!",
(March 12, 2018).

DD & Rajya Sabha TV

Conclusions

- Entropy driven extended solid solutions/point defects can scatter phonons heavily, thereby decreases the κ_{lat}.
- Intrinsic low thermal conductivity is an attractive paradigm for developing high performance thermoelectric.
- Bonding hierarchy: Coexistent of rigid covalent substructure with weakly bound ionic substructure resembling the *phonon-glass electron-crystal.*
- Large ADPs and strained lone pair as signatures of low thermal conductivity in search of new thermoelectric materials.
- Soft optical phonons generated by local vibration of selective lattice and complex crystal structure reduce the thermal conductivity.

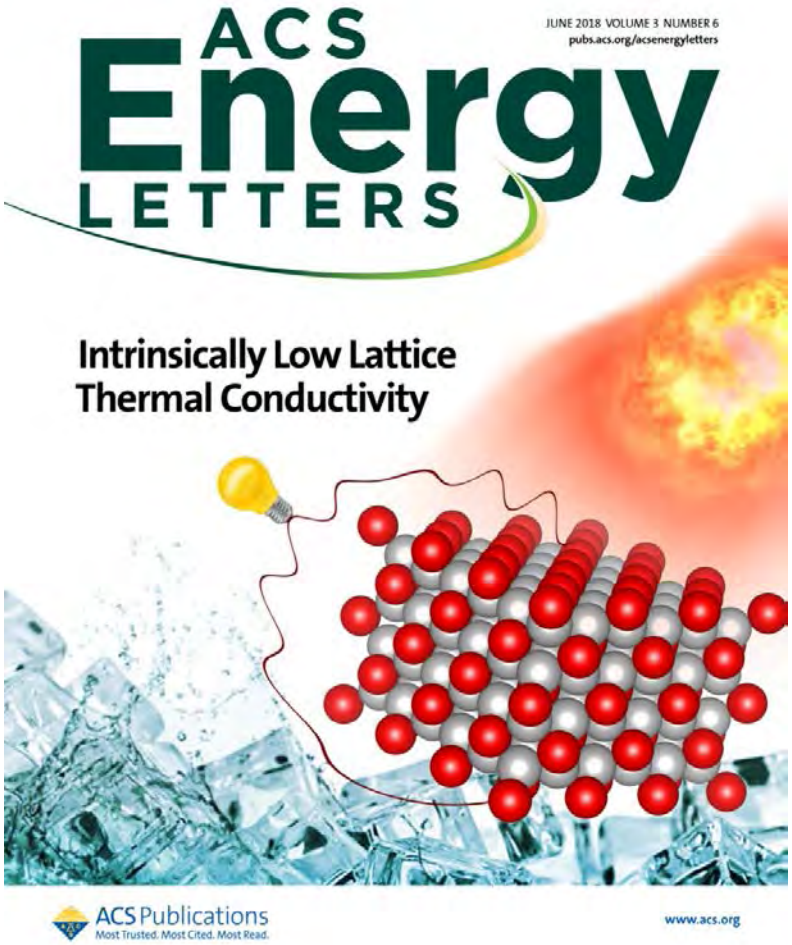

Acknowledgements

Thank you

Excellent Collaborators

- Prof. Umesh Waghmare, JNCASR
- Prof. Dirtha Sanyal, VECC, Kolkata
- Prof. Pankaj Mandal, IISER, Pune

Generous Funding

- Materials for Energy, DST, India
- Science and Engineering Board (SERB), India
- Sheiq Saqr Laboratory, JNCASR
- New Chemistry Unit, JNCASR